Trend and seasonality of land precipitation in observations and CMIP5 model simulations

Xiaofan Li[1], Zeng-Zhen Hu[2,*], Xingwen Jiang[3], Yueqing Li[3]

Zongting Gao[4], Song Yang[5], Jieshun Zhu[2,6], and Bhaskar Jha[2,6]

(1) School of Earth Sciences, Zhejiang University, Hangzhou, Zhejiang 310027, China
(2) Climate Prediction Center, NCEP/NWS/NOAA, College Park, Maryland 20740, USA
(3) Institute of Plateau Meteorology, China Meteorological Administration, Chengdu, Sichuan, China
(4) Institute of Meteorological Sciences of Jilin Province, and Laboratory of Research for Middle-High Latitude Circulation and East Asian Monsoon, Changchun 130062, China
(5) School of Environmental Science and Engineering, Sun Yat-sen University, Guangzhou 510275, China
(6) Innovim, LLC, Greenbelt, MD, USA

International J. Climatology (re-revised)

Corresponding author address:
Zeng-Zhen Hu
Climate Prediction Center

This is the author manuscript accepted for publication and has undergone full peer review but has not been through the copyediting, typesetting, pagination and proofreading process, which may lead to differences between this version and the Version of Record. Please cite this article as doi: 10.1002/joc.4592

NCEP/NWS/NOAA
5830 University Research Court
College Park, Maryland 20740
Zeng-Zhen.Hu@NOAA.GOV

Abstract

In this study, we examined the annual precipitation amounts, the seasonality over global land and their linear trends, as well as the uncertainties in two observations (precipitation reconstruction (PREC), and Global Precipitation Climate Centre (GPCC)), and then compared them with historical runs by multiple models. Overall, the large-scale patterns of both the climatology of the annual precipitation amount and the seasonality are consistent between the two observations. Nevertheless, some noticeable differences existed, particularly in the regions with fewer gauge observations, such as northern Africa and the Tibetan Plateau. For long-term changes, significant drying trends during 1948–2005 were observed in the tropical areas of northern Africa, accompanied by significant wetting trends in the polar region of Canada. The seasonality change during the period was dominated by a decreasing trend in precipitation, especially in the western portion of Russia.

The model simulations of the Coupled Model Intercomparison Project, Phase 5 (CMIP5) reproduced the climatological mean state of annual precipitation and its seasonality in the observations, as well as to some extent the zonal mean trends of precipitation amounts, but did not reproduce the zonal mean trends of seasonality. The two-dimensional distribution of linear trends of annual precipitation and seasonality simulated by CMIP5 models showed little consistency with their observational counterparts. One possibility for the inconsistencies was that they were largely determined by internal variations of the climate system rather than external forcings. In contrast, it might also suggest a challenge for state-of-the-art climate models to correctly simulate the spatial distribution of responses of annual precipitation amounts and seasonality to the evolution of external forcings. Our results suggest that, in addition to the precipitation amount, seasonality should be used as a metric to assess the ability of a climate model to simulate current climate conditions and project future climate change.

Key Words: land precipitation; mean and seasonality; climatology and trend; observations and

CMIP5

Running Head: simulated and observed precipitation seasonality and change

1. Introduction

Precipitation and surface air temperatures are the two key elements that are widely used to measure the Earth's climate, including its variability and change (Wallace and Hobbs, 2006). Observed surface air temperature changes during the instrumental period have been documented in literature with consensus results achieved (e.g., Chapter 11 of IPCC, 2013). Projections for future temperature increases in warmer climates have been achieved with high confidence (Chapter 11 of IPCC, 2013). In contrast, changes in the observed precipitation are less consistent among various observation-based datasets (e.g., Chapter 11 of IPCC, 2013), which may be attributed to limited gauge observations, as well as the more significant regional features and larger temporal variability of precipitation compared with those of surface air temperatures. Balan Sarojini et al. (2012) speculated that extensive and significant changes in precipitation over land and ocean may have already occurred, though inadequacies in the observations in some parts of the world make it difficult to conclusively identify such a human fingerprint on the global water cycle. For example, observed global ocean surface salinity changed for the time period 1950–2000 combined with changes from global climate models suggest that a robust intensification of the global water cycle occurred at a rate of 8±5% per degree of surface warming (Durack et al., 2012). Moreover, projections for future precipitation changes in warmer climates have lower confidence compared with those for surface air temperatures, particularly at regional scales (Deser et al., 2012; Hu et al., 2012; Chapter 11 of IPCC, 2013; Huang et al., 2014; Gu et al., 2015; Palomino-Lemus et al., 2015; Sun et al., 2015; Vera and Diaz, 2015). Moreover, the different confidences in the future projections of surface air temperatures

and precipitation in warmer climates appear to be largely due to the uncertainty differences caused by internal variability (Deser et al., 2012). For example, the changes in surface air temperature could be detected earlier and with fewer ensemble members compared to changes in precipitation due to their differences in internal variability. In contrast, the lower confidence of precipitation projections is associated with large internal variability of precipitation in nature, as well as the sensitivity of precipitation to the physics in climate models. For example, Stevens and Bony (2013) noted that precipitation responses to warming critically rely on the model used, suggesting the importance of coupling between atmospheric water and circulation in precipitation projections.

In addition to the change of annual precipitation amounts, the seasonal or monthly distribution of annual precipitation amounts within a year also has significant consequences. For example, if below normal (or above normal) precipitation amounts happen over an extended period of time, drought (or flood) conditions may follow. Thus, seasonality is an important measurement for the climate feature of precipitation in observations (Walsh and Lawler, 1981; Hu et al., 2003; Pascale et al., 2015) and in climate model simulation assessments (Pascale et al., 2015). Due to the shortage of observational data and large internal variability, the change in the observed precipitation seasonality over global land has not been well documented (Pascale et al., 2015). Its future projections in warmer climates have tremendous divergence (Chapter 11 of IPCC, 2013). Recently, Pascale et al. (2015) proposed two new indicators for rainfall seasonality based on information entropy, relative entropy, and a dimensionless seasonality index and evaluated the mean seasonality and differences/biases on global and regional scales in observations (Climatic Research Unit (CRU)

and Global Precipitation Climate Centre (GPCC)) and historical simulations from coupled atmosphere–ocean general circulation models (CGCMs). They noted some differences in the total precipitation amount and its seasonality between the two observational datasets, as well as pronounced divergences and biases in the simulations by the CGCMs from the Coupled Model Intercomparison Project, Phase 5 (CMIP5).

In this study, based on both observational datasets and multi-model simulations, we first analyzed the observed annual precipitation and seasonality climatologies in addition to their linear trends, with a focus on the global spatial pattern with significant regional features and the possible uncertainties. Then, we compared the observations with the historical runs by 10 CMIP5 models. It was expected that through analysis and comparison, we could identify the observed seasonality and precipitation amount changes and thus assess the ability of state-of-the-art models to simulate the observed precipitation amounts and climatological features of the seasonality as well as their changes (trends). The study is organized as follows. The data used in this work from observations and model simulations, as well as the seasonality measurements, are introduced in Section 2. The climatologies of annual mean precipitation amounts and seasonality, as well as their linear trends, are described in Section 3. In Section 4, we compared the observed features with the model simulations. Conclusions with some discussion are given in Section 5.

2. Data and Seasonality Measurement

Considering the uncertainties in precipitation records (e.g., Balan Sarojini et al. 2012; Bindoff

et al. 2013; Hegerl et al. 2015; Pascale et al. 2015), particularly during earlier periods with limited gauge observations, two analyzed precipitation datasets were used in this study. The first set is the precipitation reconstruction dataset (PREC; Chen et al., 2002) covering an extended period from 1948 to the present. The global analyses in this set were defined by the optimal interpolation of gauge observations over land, which includes gauge observations from over 17,000 stations collected in the Global Historical Climatology Network, version 2 (GHCN2), and the Climate Anomaly Monitoring System datasets. The second set is the full data reanalysis version 6.0 of Global Precipitation Climate Centre over land (GPCCv6; Schneider et al. 2011, 2014). The GPCCv6 covers the period from 1901 to 2010, based on quality-controlled data from 67,200 stations worldwide that feature data recorded for durations of 10 years or longer (Schneider et al. 2011, 2014). The two precipitation datasets had the same spatial resolution (1° × 1°).

The monthly mean precipitation data from the historical runs of 10 CMIP5 models (obtained from http://cmip-pcmdi.llnl.gov/cmip5/; Taylor et al. 2012; Jha et al. 2014) totaled 50 ensemble members and were compared with the above two precipitation datasets over the period from January 1948 to December 2005. In the historical runs, models (fully CGCMs) were forced by the specification of time evolving the observed solar, volcanic, and anthropogenic forcings from 1870 to 2005. Detailed information about the models including the institutions where the models were run, model versions, horizontal resolutions, number of ensemble members, and acronyms of the model centers is listed in Table 1 or can also be found on the website http://pcmdi3.llnl.gov/esgcet/home.html. To compute the multi-model ensemble, all model data were bilinearly interpolated into the lowest resolution among

the 10 models (see Table 1), resulting in a unified grid of 128 (zonal) × 64 (meridional). The observational data were also interpolated into the unified grid for comparison.

The annual mean climatology and the seasonality of precipitation amounts over land were analyzed, and the linear trends in both annual precipitation and seasonality in the observations and model simulations were examined and compared. To display the divergence of the model simulations, spreads of the model simulated precipitation and seasonality climatologies as well as linear trends were examined.

Following Walsh and Lawler (1981), the seasonality of precipitation was measured by the following formula:

$$\mathrm{SI} = \frac{1}{R}\sum_{i=1}^{i=12} \left| r_i - \frac{R}{12} \right| \quad (1)$$

where R is the annual precipitation amount, and r_i is the monthly mean precipitation amount in month "i". The SI value was computed by using observation-based precipitation, as well as the precipitations from the 10 CMIP5 models. Theoretically, SI can vary from zero (if all the months have an equal precipitation amount) to 1.83 (if the annual precipitation falls in a single month) (Walsh and Lawler, 1981). A larger (or smaller) SI value refers to a stronger (or weaker) variation of precipitation from one month to another within a given year.

3. Climatologies and Trends of Observations and Uncertainties

3.1 Precipitation and seasonality climatologies in the observations

Prior to examining the seasonality, we first analyzed the annual precipitation amount climatology in PREC and GPCC (Figs. 1a, 1b). It was noted that abundant precipitation occurred over the tropical areas of Africa and in southeastern Asia, northern South America, southeastern United States, and Caribbean Sea regions. Deficient precipitation occurred over a broad region from northern Africa to central Asia as well as in the high latitudes of the Northern Hemisphere (NH) and some mid-latitude regions of the Southern Hemisphere (SH). The mean annual precipitation amount was less than 100 mm in northern Africa, part of the Middle East, and between central Asia and northwestern China. The spatial distribution pattern of annual precipitation climatology (Figs. 1a, 1b) is well known (e.g., New et al., 1999; Fig. 1a of Pascale et al. 2015). The similarity of the large scale pattern between PREC (Fig. 1a) and GPCC (Fig. 1b) may imply the reliability of the observational records in describing the climatological precipitation amounts. However, the similarity could be partially due to the fact that both PREC and GPCC used similar raw data and analysis approaches. For example, a large volume of gauge observations from GHCN2 is used in both PREC and GPCC (Chen et al. 2002; Schneider et al. 2014), and the observations from gauge stations are similarly interpolated into regular grid points. Nevertheless, some differences between PREC and GPCC (Figs. 1c, 1d) existed at regional scales. The relative differences were especially pronounced in northern Africa, the Tibetan Plateau, and central Asia, with amplitudes larger than 20% (Fig. 1d). The collocation with regions having a shortage of gauge observations (see Fig. 5 of Schneider et al. 2014) may imply that the quantity of gauge observations impacted the interpolation from gauge stations to regular grid points.

Climatologically, small seasonalities were observed in Europe, North America, and tropical landmasses, whereas large seasonalities occurred in regions from northern Africa to central Asia, Mongolia, northeast China, and part of the subtropical SH (Figs. 2a, 2b). The spatial pattern of seasonality was generally consistent with that shown in previous studies for global (e.g., Fig. 1c of Pascale et al. 2015) or regional domains (such as East China, Fig. 4 of Hu et al. (2003); Africa, Fig. 2 of Walsh and Lawler (1981)). Although differences were present in some regions, such as in northern Africa and the Tibetan Plateau (Figs. 2c, 2d), the overall spatial patterns of the climatological seasonality were similar between PREC and GPCC (Figs. 2a, b), suggesting the consistency of the two observational datasets in describing the large scale distribution of the climatological seasonality.

Interestingly, the spatial distribution pattern for seasonality climatology (SI value) was analogous to that of the annual precipitation amount climatology in most regions (Figs. 1a, 1b, 2a, 2b). That is, abundant (deficient) precipitation collocated with small (large) seasonality, suggesting that less (more) precipitation generally favored larger (smaller) seasonality. However, this kind of relation did not hold for the northern part of North America where both the annual precipitation amount and the seasonality were relatively small and in northeastern Siberia where both were relatively large. The reasons behind the relation between the annual precipitation amount climatology and seasonality climatology, as well as the regional dependence of the relationship, were not immediately apparent.

3.2 Precipitation and seasonality trends in the observations

For the long-term trends of annual precipitation amounts in the observations during 1948–2005 (Fig. 3a), significant and large-scale drying tendencies were observed in the tropical regions of northern Africa, whereas significant and large-scale wetting tendencies were seen in the polar region of Canada, and in central and western Australia. The drying tendencies in northern Africa within 5°N–20°N seemed to be associated with the meridional migration of the dry zone in the Sahara region and expansion of the desert (Nicholson 2013). For the Asian summer monsoon region, both drying and wetting trends were observed. In northern South America and middle-high latitudes of NH, the spatial distribution showed many small spatial scale features without any large-scale significant trends.

To highlight the regional long-term trends, Figs. 3b and 3c show the monthly mean anomalies of precipitation averaged in the tropical region of North Africa (5°N–20°N, 15°W–35°E) and the polar region of Canada (60°N–80°N, 115°W–65°W) (see the rectangles in Fig. 3a for the domains), respectively. A drying (wetting) tendency was observed from the average in tropical North Africa (the polar region of Canada), and these features were consistent with the results shown in Fig. 3a. However, although the large scale patterns of the linear trends were generally similar between PREC and GPCC (Fig. 3a), some notable differences were evident. For example, the wetting trends in central Europe were significant for GPCC but not for PREC. Furthermore, the wetting trends in the polar region of Canada (Figs. 3a, 3c) were more significant in PREC than in GPCC.

Compared to the trends in the annual precipitation amounts, the trends in seasonality were mostly negative (Fig. 4a). Negative trends were significant over the western portion of Russia,

whereas positive trends were observed in part of Canada for both PREC and GPCC. However, there were also clear differences between PREC and GPCC in some regions, such as central Asia, southern Africa, and Australia.

To examine the regional details of the seasonality trend, Figs. 4b and 4c as two examples show the seasonal cycles in the western part of Russia (55°N–75°N, 65°E–95°E) and central Canada (50°N–60°N, 120°W–85°W) based on two equal-length periods from January 1948 to December 1976 (dashed and green line), and from January 1977 to December 2005 (solid and red line) (see the rectangles in Fig. 4a for the domains), respectively. For the western part of Russia, the decreasing trend in seasonality was caused by a combination of the decrease in precipitation in the summer months and the increase in precipitation in the winter months (by comparing the dashed/green line with the solid/red line in Fig. 4b). The reduced amplitude of the seasonal cycle corresponded to a decrease in seasonality. In contrast, the seasonality increase in central Canada was mainly caused by a decrease in precipitation in the winter months, as the precipitation change was less pronounced in the summer months (Fig. 4c). The increase in the range of precipitation amounts in winter and summer months resulted in an increase of the seasonality in central Canada. These seasonality changes were expected to connect with large-scale atmospheric circulation changes, which deserve further investigation.

Overall, the large-scale patterns of both climatologies of the annual mean precipitation amounts and seasonality were consistent between the two observational datasets. Nevertheless, some noticeable differences existed, particularly in regions with limited gauge observations, such as

northern Africa and the Tibetan Plateau. These may be associated with multipole factors, such as some differences of raw data as well as the detailed analysis approaches used in PREC and GPCC (Chen et al. 2002; Schneider et al. 2014). For long-term changes, drying trends in the tropical regions of northern Africa and wetting trends in the polar region of Canada were significant in both observations. The seasonality change of the observed precipitation during 1948–2005 was dominated by decreasing trends, especially in the European portion.

4. Comparison of Model Simulations with the Observations

4.1 Precipitation and seasonality climatologies in the model simulations

The large-scale spatial patterns of climatological means of annual precipitation amounts and seasonality in the observations (Figs. 1a, 1b, 2a, 2b) were captured in the average of the historical runs of the multi-model and multi-ensemble members (Figs. 5a, 6a). Nevertheless, in addition to the amplitude discrepancies in some regions (Figs. 5b, 5c, 6b, 6c) between the model mean and observations, the spatial pattern was smoother in the model simulations (Figs. 5a, 6a) than in the observations (Figs. 1a, 1b, 2a, 2b).

Furthermore, compared with the observations (here referred to as the mean of PREC and GPCC), some regional features were not well simulated. For example, the annual precipitation amount climatology in the CMIP5 models tended to be overestimated, particularly in the Tibetan Plateau, western North America, northern Africa, and Australia (Fig. 5b). In contrast, it was underestimated in Saudi Arabia, most of the Indian Peninsular, and central South America (Fig. 5b).

The annual precipitation amount climatology in the Tibetan Plateau, western North America, subtropical northern Africa, and Australia was overestimated by 50% or more (Fig. 5c). On the contrary, an underestimation of the annual precipitation amount climatology was confined to relatively smaller areas and its amplitude was mostly smaller than 30%. The most pronounced differences appeared to be co-located with highland areas, such as the Tibetan Plateau in Asia, the Rocky Mountains in North America, and the Andes Mountains in South America (Figs. 5b, 5c). These regions also had relatively fewer gauge observations (see Fig. 5 of Schneider et al. 2014), which may imply a defect of the observations, but also possibly suggests a challenge for climate models in simulating precipitation over these complex topographical regions (Figs. 5b, 5c). The spatial pattern of model spread well followed that of the annual precipitation amount climatology, where large (small) spreads corresponded to large (small) annual precipitation amount (Figs. 5a, 5d). Here, the model spread is referred to as the square root of individual model simulations referenced to the all model mean.

The difference between simulated and observed seasonality climatologies (Figs. 6b, 6c) displayed an overall similar spatial pattern to that of the difference between simulated and observed annual precipitation amount climatologies (Figs. 5b, 5c). That is, overestimated (underestimated) seasonality climatology corresponded to overestimated (underestimated) annual precipitation amount climatology. The amplitudes of the differences reached 10%–50% of the observed seasonality climatology (Fig. 6c). Similar to the corresponding relationship between the annual precipitation amount climatology and its spread among models, a large (small) spread of the seasonality among

the models was associated with large (small) seasonality climatology (Figs. 6a, 6d). These similarities may imply that the seasonality was largely determined by extreme amounts of precipitation, e.g., during the extremely dry and wet months within a year according to the SI formula (see equation (1)).

4.2 Precipitation and seasonality trends in the model simulations

For the linear trend of annual precipitation amounts during 1948–2005, there were few similarities of the two dimensional distribution between the observations (PREC or GPCC) and the average of model simulations (Figs. 3a, 7a). The differences of the trends between the simulations and observations (Figs. 7c, d) were large, especially in tropical Africa, Asia, southeastern Canada, part of Europe, and South America. Interestingly, the zonal averaged trends in the observations were qualitatively captured to some extent by some models, as well as by the all model mean (Fig. 8). For example, the drying trends in the tropics and along 45°S and the wetting trends in 30°S–40°S were qualitatively similar between the model mean and the two observations, although the amplitudes were much smaller in the model mean than in the observations. This is consistent with results from Nasrollahi et al. (2015), who reported that CMIP5 models are generally consistent with observed (CRU) drying and wetting trends at a global (or hemispheric) scale, but most models have difficulties capturing the regional distributions of observed drying and wetting trends. The overall spread of the linear trends of annual precipitation amounts among models was more pronounced in SH than in NH in the current study (Fig. 7b).

The differences of the seasonality trends during 1948–2005 between observations and model simulations were even more notable for both the spatial pattern and amplitude (Figs. 4a, 9a, 9c, 9d). On average, the seasonality trends in the models were much smaller than those in the observations (Figs. 4a, 9a, 9c, 9d), and the spreads among the models were quite large (Fig. 9b). The smaller amplitudes of the trends in the simulations may have been partially due to the average and cancelation among the models. Different from the zonal averaged linear trends of precipitation with reasonable simulations, the models were unable to capture the observed zonal averaged linear trends of their seasonality. In fact, the zonal averaged linear trends of seasonality also displayed obvious differences between PREC and GPCC (Fig. 10a). For instance, the zonal mean linear trend of precipitation seasonality was clearly all negative in PREC between 40°S and 30°N (red dot curve in Fig. 10a), but it fluctuated around zero in GPCC (green dash curve in Fig. 10a). The differences between PREC and GPCC became even larger between 40°S–55°S. This results in a challenge for monitoring the seasonality change based on the available observation records.

In summary, the mean state of the annual mean precipitation amounts and seasonality are fairly good simulated. Furthermore, to some extent, the model average qualitatively reproduced the observed zonal mean precipitation trends but not the seasonality trends. There were pronounced differences in the spatial distributions of the linear trends of both the precipitation amounts and the seasonality between the simulations and observations. The disagreements of the linear trends of the annual precipitation amounts and the seasonality between the observations and model simulations may have two implications. Firstly, the spatial distribution of the observed annual precipitation

amounts and seasonality trends may not have been the result of external forcings (e.g., increases of greenhouse gas (GHG) concentrations and time evolution of solar-volcanic forcing). It may possibly have been caused by internal dynamics of the atmosphere and ocean. Secondly, the climate models may have been unable to simulate the realistic spatial pattern of the response of the annual precipitation amounts and seasonality changes to these time evolution forcings, suggesting a challenge for the state-of-the-art CGCMs. Furthermore, another important reason that may have resulted in the differences between the models and observations is the fact that precipitation in models is sensitive to the parameterization schemes of the precipitation, clouds, and other associated physical processes.

5. Summary

In this study, we examined the climatologies of the annual precipitation amount and its seasonality over global land, their linear trends in observations, and their uncertainties and compared them with historical runs of multiple CMIP5 models. The large scale patterns of both climatologies of annual mean precipitation amounts and seasonality were almost identical between two observational datasets. Nevertheless, some differences were evident, particularly in regions with limited gauge observations such as in northern Africa and the Tibetan Plateau. For long-term changes, significant drying trends during 1948–2005 were observed in the tropical regions of northern Africa, which were accompanied by significant wetting trends in the polar region of Canada. The seasonality change of the observed precipitation during 1948–2005 was dominated by decreasing trends,

especially in the western portion of Russia.

The model simulations well captured the spatial pattern and intensity of annual precipitation amounts and the seasonality climatologies of the observations, as well as, to some extent, the zonal mean of precipitation trends but not the zonal mean of seasonality trends. Furthermore, the model-simulated two-dimensional spatial distribution of linear trends of both the annual precipitation amount and its seasonality showed little consistency with the corresponding trends in the observations. The disagreements of the two dimensional distribution of both annual precipitation amounts and seasonality linear trends between the observations and historical runs of the multi-model simulations may imply that the two dimensional distribution of observed trends may not be determined by external forcings, but could be due to the low-frequency internal variation of the climate system. That is different from the attribution for long-term trends of surface air temperatures, which are largely due to the increases of GHG concentrations (Chapter 10 of IPCC, 2013). In contrast, it also provides a challenge for the state-of-the-art CGCMs to correctly simulate the spatial distribution of responses of annual precipitation amounts and seasonality to the time evolutions of external forcings (e.g., increases in GHG concentrations and the time evolution of solar-volcanic forcing). The feature challenges the fidelity of future projections under different scenarios (Chapter 11 of IPCC, 2013).

Our analysis suggested that, in addition to the annual precipitation amount, seasonality could be an additional metric to assess the ability of climate model in simulating the current climate and in projecting future climate change. This metric could serve as a higher order and provide more strict

criteria for the model assessment and also for observational quality verification.

Due to the shortage of gauge observations in the early period of the observational records analyzed in this study, as well as the heterogeneous distributions of gauge observations in both spatial and temporal domains, some local features may be affected by these factors, particularly for the linear trends of the precipitation and the seasonality (e.g., Balan Sarojini et al. 2012; Bindoff et al. 2013; Hegerl et al. 2015; Pascale et al. 2015). For example, Pascale et al. (2015) noted that different land observational datasets reveal substantial differences in their representation of seasonality. In terms of the model simulations, although different models may have substantial differences, a grand ensemble with 10 models and a total of 50 ensemble members should give quite robust results. More importantly, due to large uncertainties in simulating linear trends of the precipitation over land and the seasonality in the models, in future, it will be necessary to examine the performance of each individual model in order to understand why some models' simulations are better than others and what the underlying physics are behind the differences in model performance.

Acknowledgements. We thank the reviewers for their constructive suggestions, which led to a significant improvement of the paper quality. This work was jointly supported by the National Natural Science Foundation of China (Grants 91337107, 41375081, and 41475039). We acknowledge the World Climate Research Programme's Working Group on Coupled Modelling, which is responsible for CMIP (http://pcmdi3.llnl.gov/esgcet/home.html). We also thank the climate modeling groups for producing and making available their model output. For CMIP, the U.S.

Department of Energy's Program for Climate Model Diagnosis and Intercomparison provides coordinating support and leads development of software infrastructure in partnership with the Global Organization for Earth System Science Portals. The GPCC data are available from "http://www.esrl.noaa.gov/psd/data/gridded/data.gpcc.html," and PREC data are available from ftp://ftp.cpc.ncep.noaa.gov/precip/50yr/gauge/. For the data of the analysis shown in this study, please contact us via zeng-zhen.hu@noaa.gov.

References

Balan Sarojini B, Stott PA, Black E, Polson D. 2012. Fingerprints of changes in annual and seasonal precipitation from CMIP5 models over land and ocean. *Geophysics Research Letters* **39**: L21706. doi: 10.1029/2012GL053373

Bindoff NL, Stott PA, AchutaRao KM, Allen MR, Gillett N, Gutzler D, Hansingo K, Hegerl G, Hu Y, Jain S, Mokhov II, Overland J, Perlwitz J, Sebbari R, Zhang X. 2013. Detection and Attribution of Climate Change: from Global to Regional. In: Climate Change 2013: The Physical Science Basis. Contribution of Working Group I to the Fifth Assessment Report of the Intergovernmental Panel on Climate Change [Stocker TF, Qin D, Plattner G-K, Tignor M, Allen SK, Boschung J, Nauels A, Xia Y, Bex V, Midgley PM (eds.)]. Cambridge University Press, Cambridge, United Kingdom and New York, NY, US

Chen M, Xie P, Janowiak JE, Arkin PA. 2002. Global land precipitation: A 50-yr monthly analysis based on gauge observations. *Journal of Hydrometeorology* **3**: 249–266.

Deser C, Phillips A, Bourdette V, Teng H. 2012. Uncertainty in climate change projections: The role of internal variability. *Climate Dynamics* **38 (3-4)**: 527-546. doi: 10.1007/s00382-010-0977-x.

Durack PJ, Wijffels SE, and Matear RJ. 2012. Ocean salinities reveal strong global water cycle intensification during 1950 to 2000. *Science* **336 (6080):** 455-458. *DOI:* 10.1126/science.1212222.

Gu HH, Yu ZB, Wang JG, Wang GL, Yang T, Ju Q, Yang CG, Xu F, Fan CH. 2015. Assessing CMIP5 general circulation model simulations of precipitation and temperature over China. *International Journal of Climatology* 35(9): 2431-2440. doi:10.1002/joc.4152.

Hegerl GC, Black E, Allan RP, Ingram WJ, Polson D, Trenberth KE, Chadwick RS, Arkin PA, Sarojini BB, Becker A, Dai A, Durack PJ, Easterling D, Fowler HJ, Kendon EJ, Huffman GJ, Liu C, Marsh R, New M, Osborn TJ, Skliris N, Stott PA, Vidale P-L, Wijffels SE, Wilcox LJ, Willett KM, Zhang X. 2015. Challenges in quantifying changes in the global water cycle.

Bulletin of the American Meteorological Society **96**: 1097–1115. doi: http://dx.doi.org/10.1175/BAMS-D-13-00212.1.

Hu Z-Z, Yang S, Wu R. 2003. Long-term climate variations in China and global warming signals. *Journal of Geophysical Research-Atmospheres* **108 (19)**: 4614. DOI: 10.1029/2003JD003651.

Hu Z-Z, Kumar A, Jha B, Huang B. 2012. An analysis of forced and internal variability in a warmer climate in CCSM3. *Journal of Climate* **25 (7):** 2356-2373. DOI: 10.1175/JCLI-D-11-00323.1.

Huang AN, Zhou Y, Zhang YC, Huang DQ, Zhao Y, Wu HM. 2014. Changes of the annual precipitation over Central Asia in the twenty-first century projected by multimodels of CMIP5. *Journal of Climate* **27(17):** 6627-6646. doi:10.1175/Jcli-D-14-00070.1.

IPCC. 2013. Climate Change 2013: The Physical Science Basis. Contribution of Working Group I to the Fifth Assessment Report of the Intergovernmental Panel on Climate Change [Stocker TF, Qin D, Plattner G-K, Tignor M, Allen SK, Boschung J, Nauels A, Xia Y, Bex V, Midgley PM (eds.)]. Cambridge University Press, Cambridge, United Kingdom and New York, NY, USA, 1535 pp.

Jha B, Hu Z-Z, Kumar A. 2014. SST and ENSO variability and change simulated in historical experiments of CMIP5 models. *Climate Dynamics* **42 (7-8):** 2113-2124. DOI: 10.1007/s00382-013-1803-z.

Nasrollahi N, AghaKouchak A, Cheng L, Damberg L, Phillip TJ. 2015. How well do CMIP5 climate simulations replicate historical trends and patterns of meteorological droughts? *Water Resource Res*earch **51**: 2847–2864. doi: 10.1002/2014WR016318.

New MG, Hulme M, Jones PD. 1999. Representing 20th century space-time climate variability. I: Development of a 1961-1990 mean monthly terrestrial climatology. *Journal of Climate* **12**: 829-856.

Nicholson NE. 2013. The West African Sahel: A Review of Recent Studies on the Rainfall Regime and Its Interannual Variability. *ISRN Meteorology* **2013**, 1-32, DOI: http://dx.doi.org/10.1155/2013/453521.

Palomino-Lemus R, Cordoba-Machado S, Gamiz-Fortis SR, Castro-Diez Y, Esteban-Parra MJ. 2015. Summer precipitation projections over northwestern South America from CMIP5 models. *Global Planet Change* **131**: 11-23. doi:10.1016/j.gloplacha.2015.05.004.

Pascale S, Lucarini V, Feng X, Porporato A, ul Hasson S. 2015. Analysis of rainfall seasonality from observations and climate models. *Climate Dynamics* **44 (11-12):** 3281-3301. DOI: 10.1007/s00382-014-2278-2.

Schneider U. Becker A, Finger P, Meyer-Christoffer A, Rudolf B, Ziese M. 2011. GPCC Full Data Reanalysis Version 6.0 at 1.0°: Monthly Land-Surface Precipitation from Rain-Gauges built on GTS-based and Historic Data. DOI: 10.5676/DWD_GPCC/FD_M_V6_100.

Schneider U, Becker A, Finger P, Meyer-Christoffer A, Ziese M, Rudolf B. 2014. GPCC's new land surface precipitation climatology based on quality-controlled in situ data and its role in quantifying the global water cycle. *Theoretical and Applied Climatology* **115 (1-2):** 15-40. DOI: http://dx.doi.org/10.1007/s00704-013-0860-x

Stevens B, and Bony S. 2013. What are climate models missing? *Science* **340 (6136),** 1053-1054. *DOI:* 10.1126/science.1237554.

Sun QH, Miao CY, Duan QY. 2015. Comparative analysis of CMIP3 and CMIP5 global climate models for simulating the daily mean, maximum, and minimum temperatures and daily precipitation over China. *Journal of Geophysics Research-Atmospheres* **120(10)**: 4806-4824. doi: 10.1002/2014JD022994.

Taylor KE, Stouffer RJ, Meehl GA. 2012. An overview of CMIP5 and the experiment design. *Bulletin of the American Meteorological Society* **93**: 485-498. doi:10.1175/BAMS-D-11-00094.1.

Vera CS, Diaz L. 2015. Anthropogenic influence on summer precipitation trends over South America

in CMIP5 models. *International Journal of Climatology* **35(10)**: 3172-3177. doi: 10.1002/joc.4153.

Wallace, JM, Hobbs PV. 2006. Atmospheric Science: An Introductory Survey, 2nd Ed., Academic Press, 504 pp.

Walsh RPD, Lawer DM. 1981. Rainfall seasonality: Description, spatial patterns and change through time. *Weather* **36**: 201-208.

Figure Captions:

Fig. 1: Climatological annual precipitation amount (mm/year) of (a) PREC and (b) GPCC. (c) The differences of PREC−GPCC and (d) the relative differences of (PREC−GPCC)/(PREC+GPCC)×100 over global land averaged in January 1948–December 2005.

Fig. 2: Climatological seasonality of (a) PREC and (b) GPCC. (c) The differences of PREC−GPCC and (d) the relative differences of (PREC−GPCC)/(PREC+GPCC)×100 over global land averaged in January 1948–December 2005.

Fig. 3: (a) Linear trend of annual precipitation amount (mm/58 years) over land during January 1948–December 2005 from the observed precipitation. The hatched regions represent the trend significant at 95% or higher confidence level using the t-test. Regional mean monthly precipitation anomaly (mm/month) in (b) the tropical North Africa (5°N–20°N, 15°W–-35°E) and (c) the northeastern Canada (60°N–80°N, 115°W–65°W) (see the rectangles in (a) for the domains). Left panels are for PREC and right ones for GPCC.

Fig. 4: (a) Linear trend of precipitation seasonality (1/58 years) over land during January 1948–December 2005 from the observed precipitation. The hatched regions represent the trend significant at 95% or higher confidence level using the T-test. Seasonal cycle of regional mean monthly precipitation anomaly (mm/month) in (b) the western part of Russia (55°N–75°N, 65°E–95°E) and (c) the central Canada (50°N–60°N, 120°W–85°W) (see the rectangles in (a) for the domains). The dashed/green (solid/red) line represents the seasonal cycle averaged in January 1948–December 1976 (January 1977–December 2005). Left panels are for PREC and right ones for GPCC.

Fig. 5: (a) Annual precipitation amount averaged for all ensemble members of all the models over land during January 1948–December 2005 (mm/year); (b) difference between the model simulation and the observation mean (PREC+GPCC)/2.0 (mm/year); (c) percentage of relative difference between the model simulation and the observation mean referred to the

observation mean (%); (d) model spread (mm/year).

Fig. 6: Precipitation seasonality averaged for all ensemble members of all the models over land during January 1948–December 2005 (mm/year); (b) difference between the model simulation and the observation mean (PREC+GPCC)/2.0 (mm/year); (c) percentage of relative difference between the model simulation and the observation mean referred to the observation mean (%); (d) model spread (mm/year).

Fig. 7: (a) Linear trend of annual precipitation amount averaged for all ensemble members of all the models over land during January 1948–December 2005; (b) model spread of the linear trend among 10 models; difference of the linear trends between (c) the model simulations and PREC and between (d) the model simulations and GPCC. The unit is mm/58 years.

Fig. 8: Zonal averaged linear trends of annual mean precipitation of (a) PREC (red dot curve), GPCC (green dash curve), and 10 model mean (black solid curve), and (b) individual models (dash curves) and 10 model mean (black solid curve). The unit is mm/58 years.

Fig. 9: (a) Linear trend of precipitation seasonality averaged for all ensemble members of all the models over land during January 1948–December 2005; (b) model spread of the linear trend among 10 models; difference of the linear trends between (c) the model simulations and PREC and between (d) the model simulations and GPCC. The unit is 1/58 years.

Fig. 10: Zonal averaged linear trends of precipitation seasonality of (a) PREC (red dot curve), GPCC (green dash curve), and 10 model mean (black solid curve), and (b) individual models (dash curves) and 10 model mean (black solid curve). The unit is 1/58 years.

Table Caption:

Table 1: Information about the CMIP5 models used in this study.

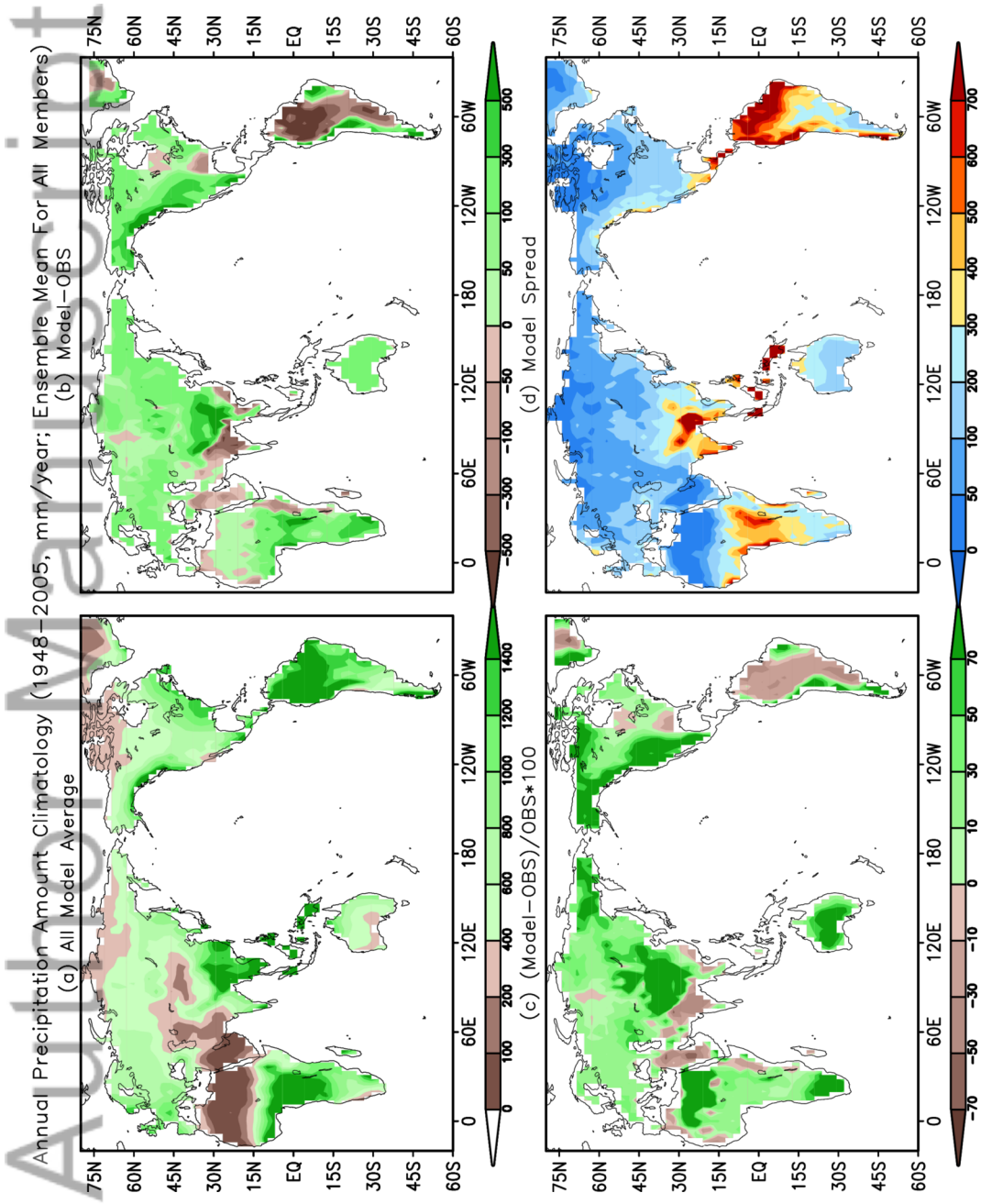

x0_cmip5_all01

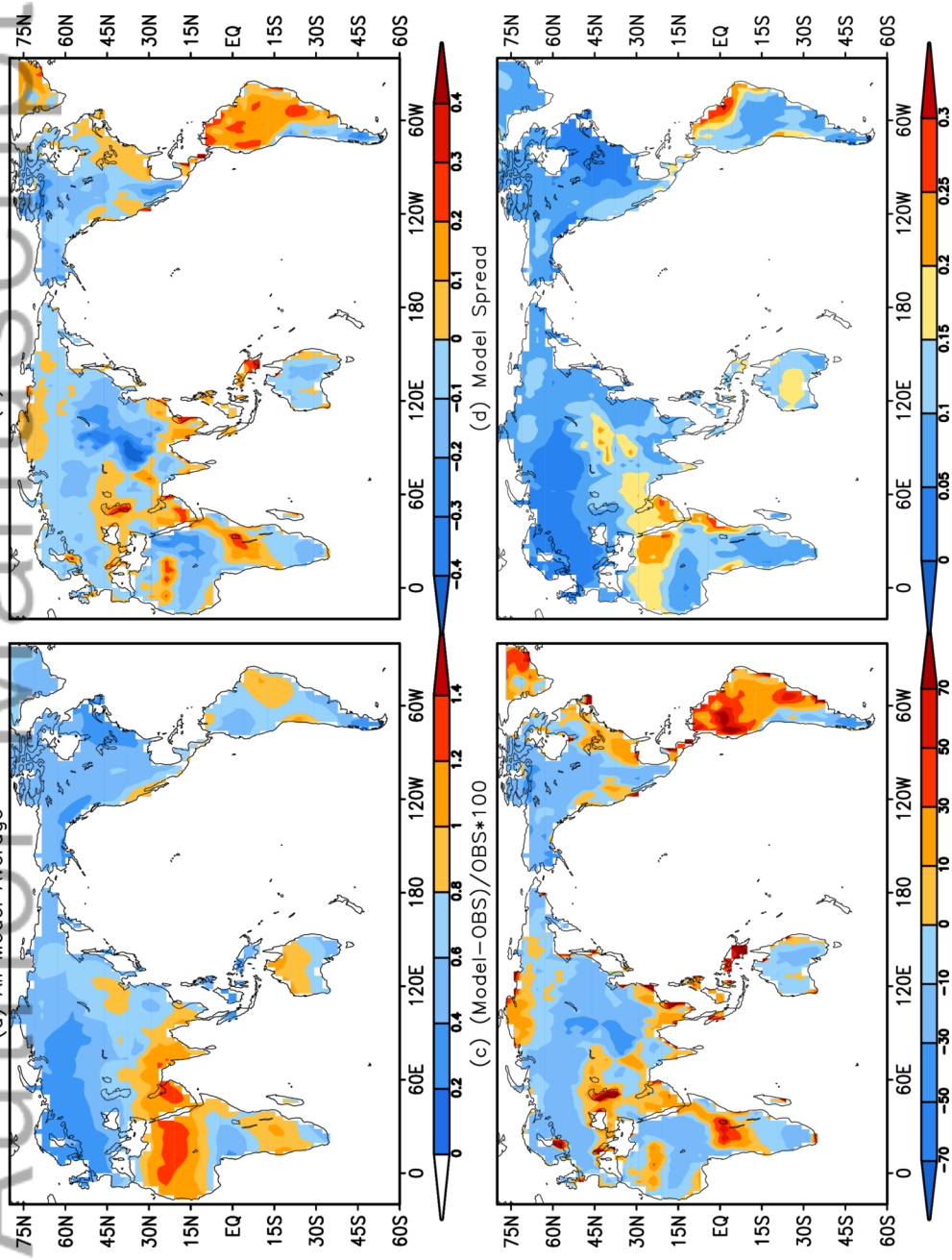

x0_cmip5_all02

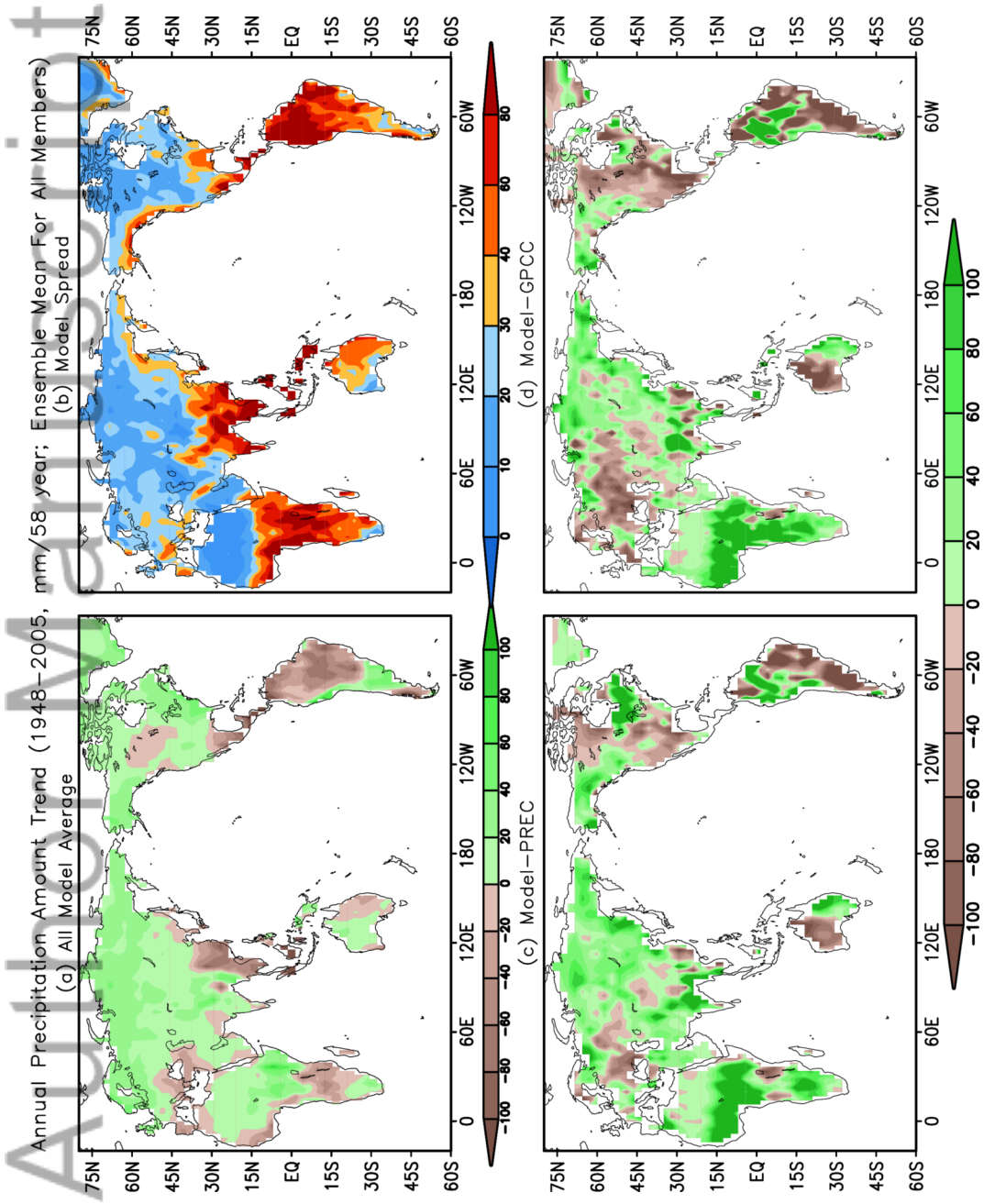

x0_cmip5_all03

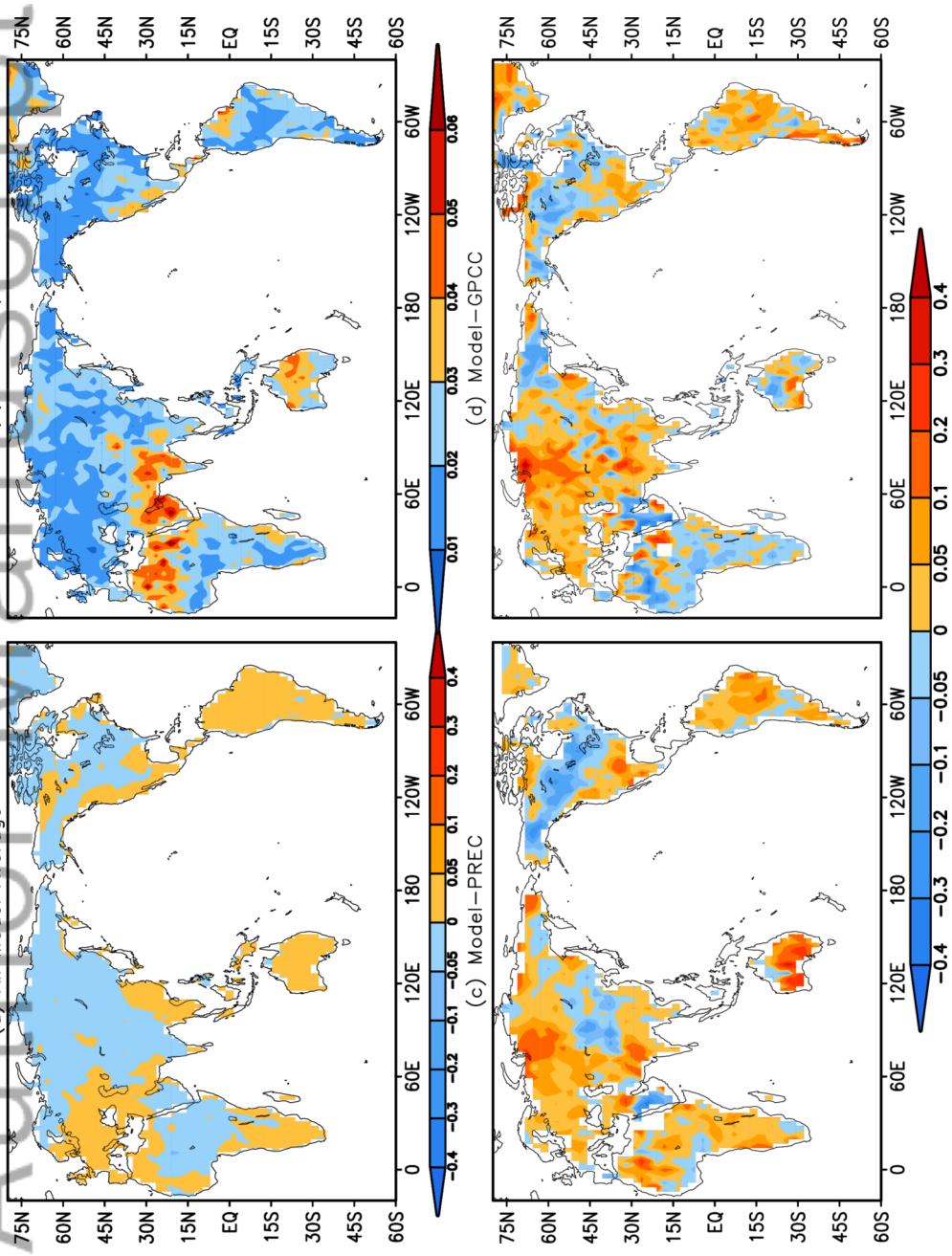

x0_cmip5_all04

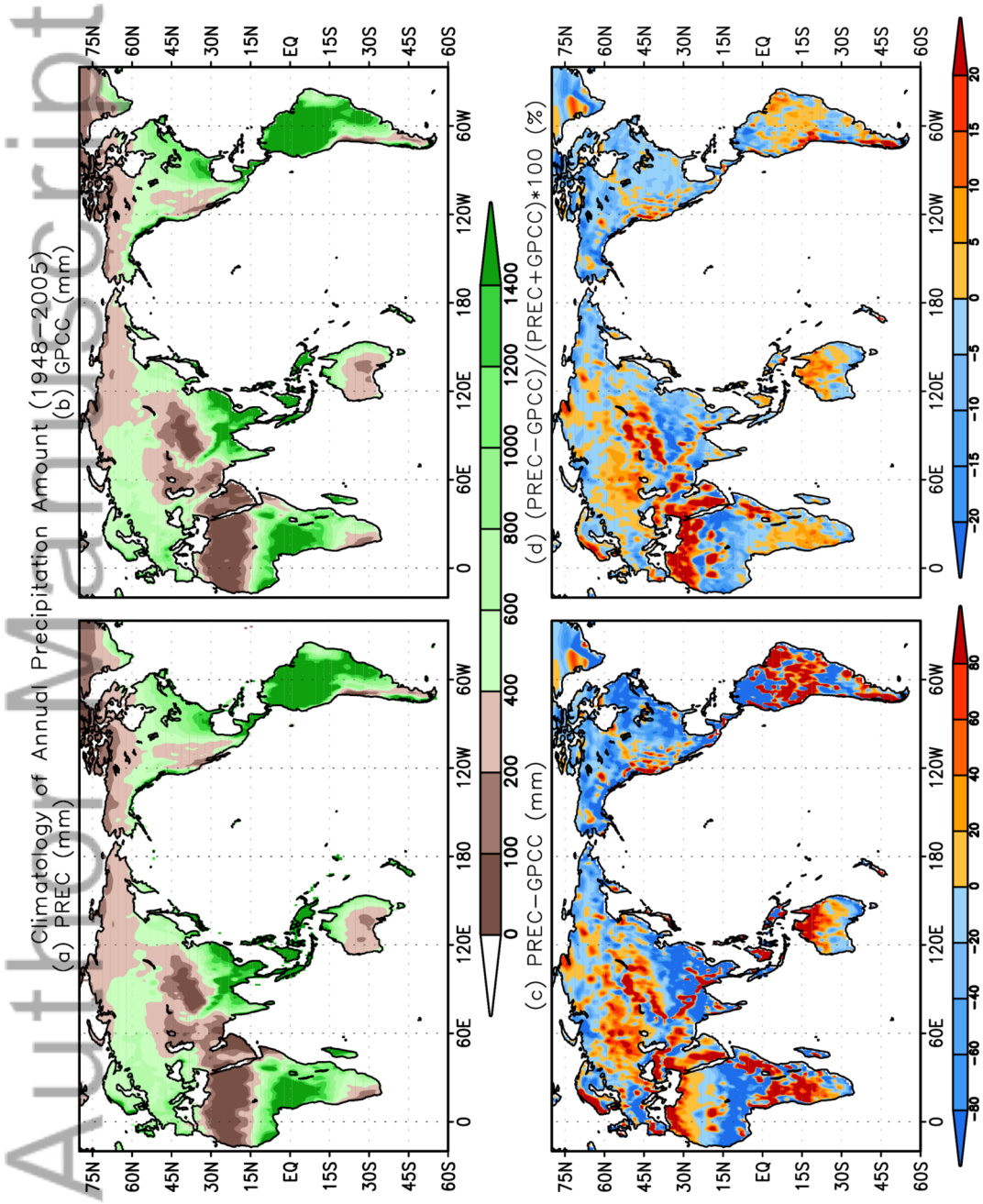

x0_obs_seasonality00

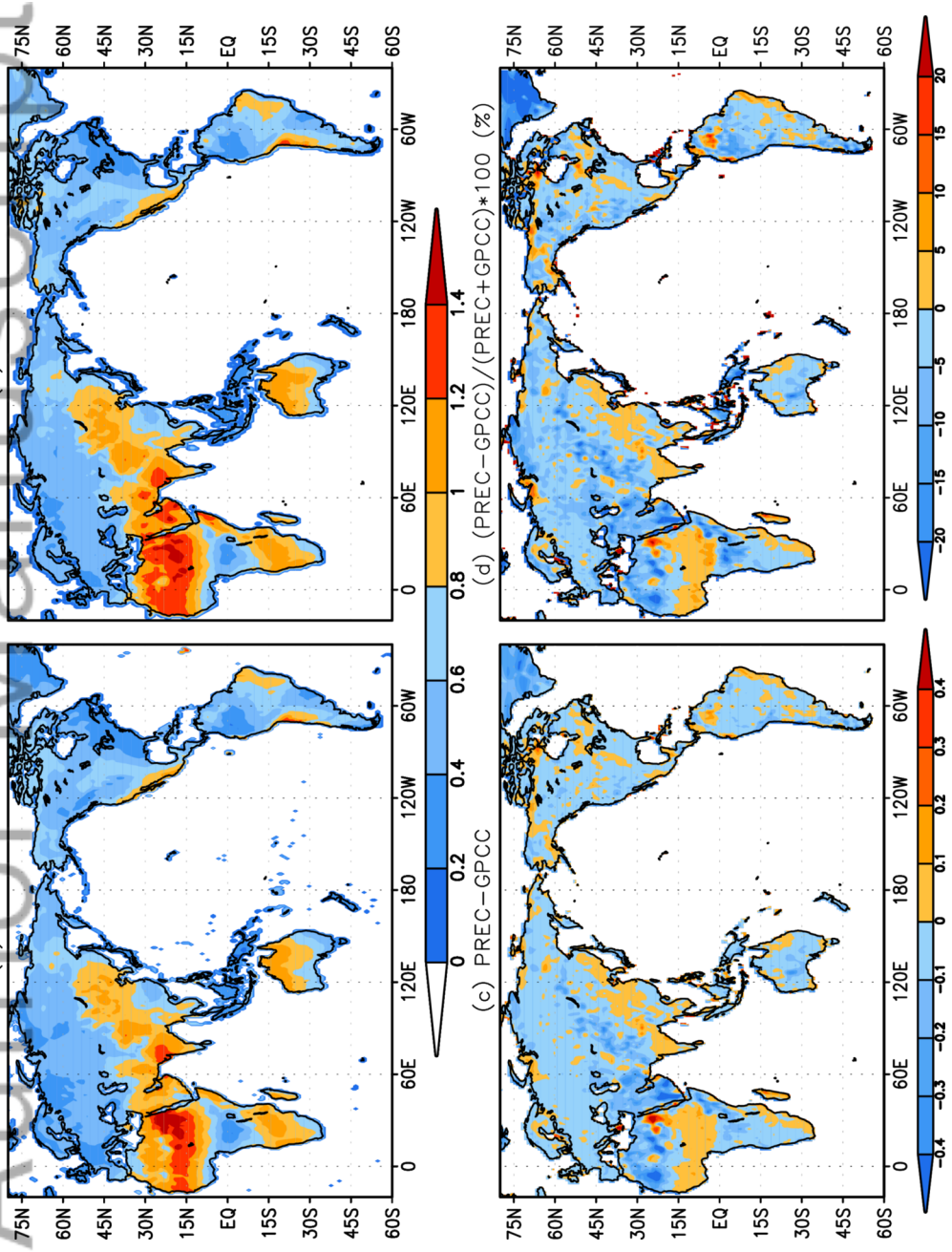

x0_obs_seasonality02

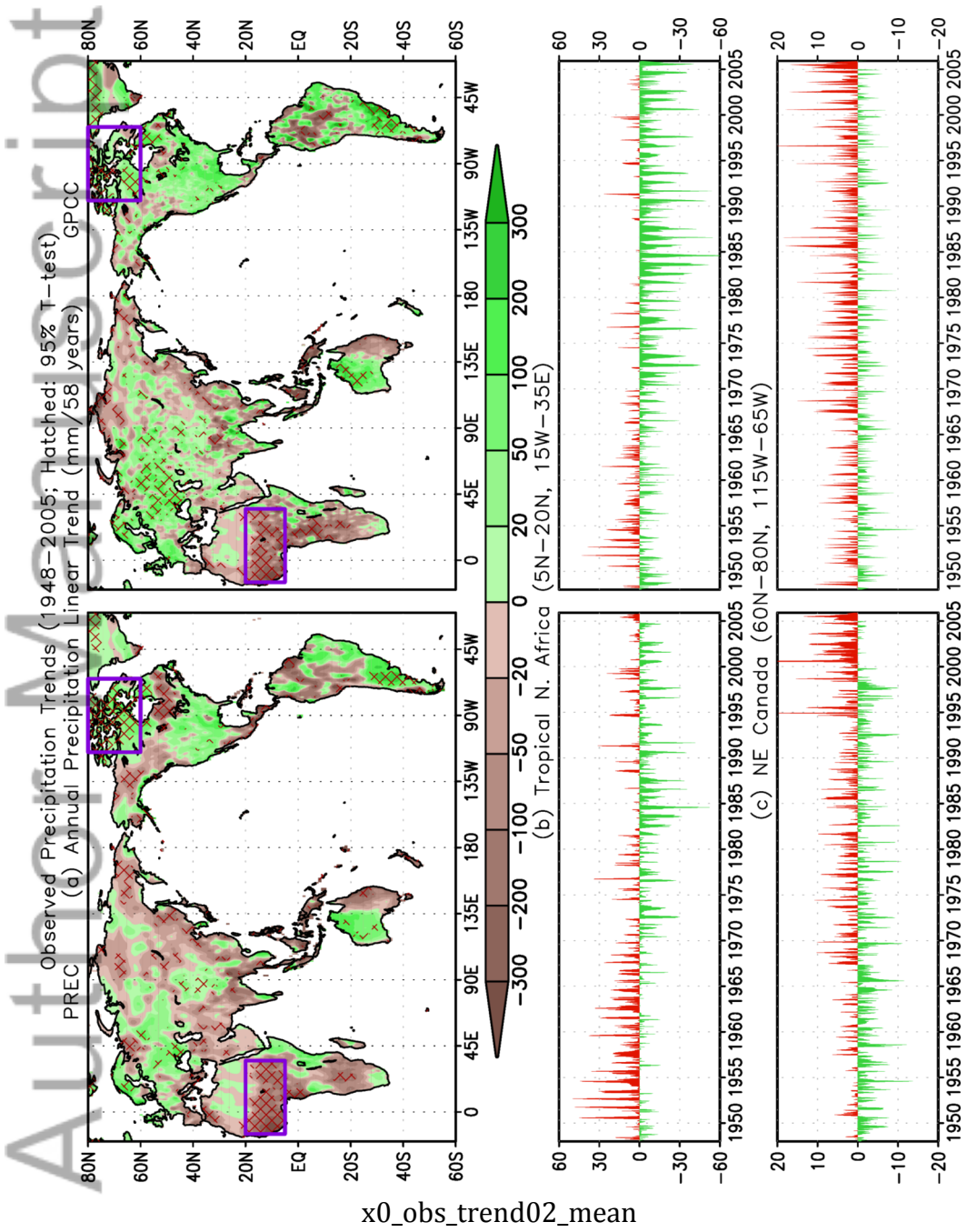

x0_obs_trend02_mean

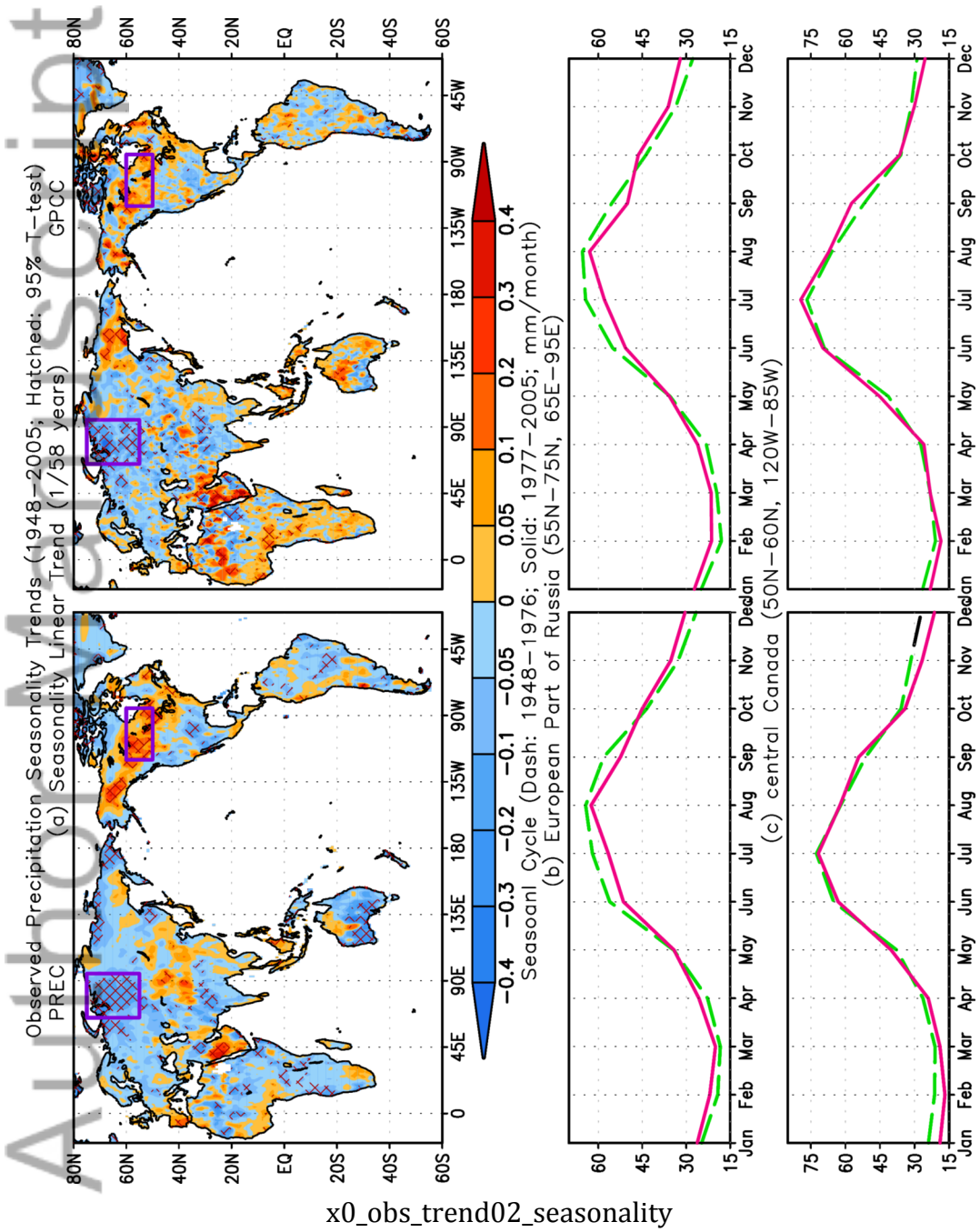

x0_obs_trend02_seasonality

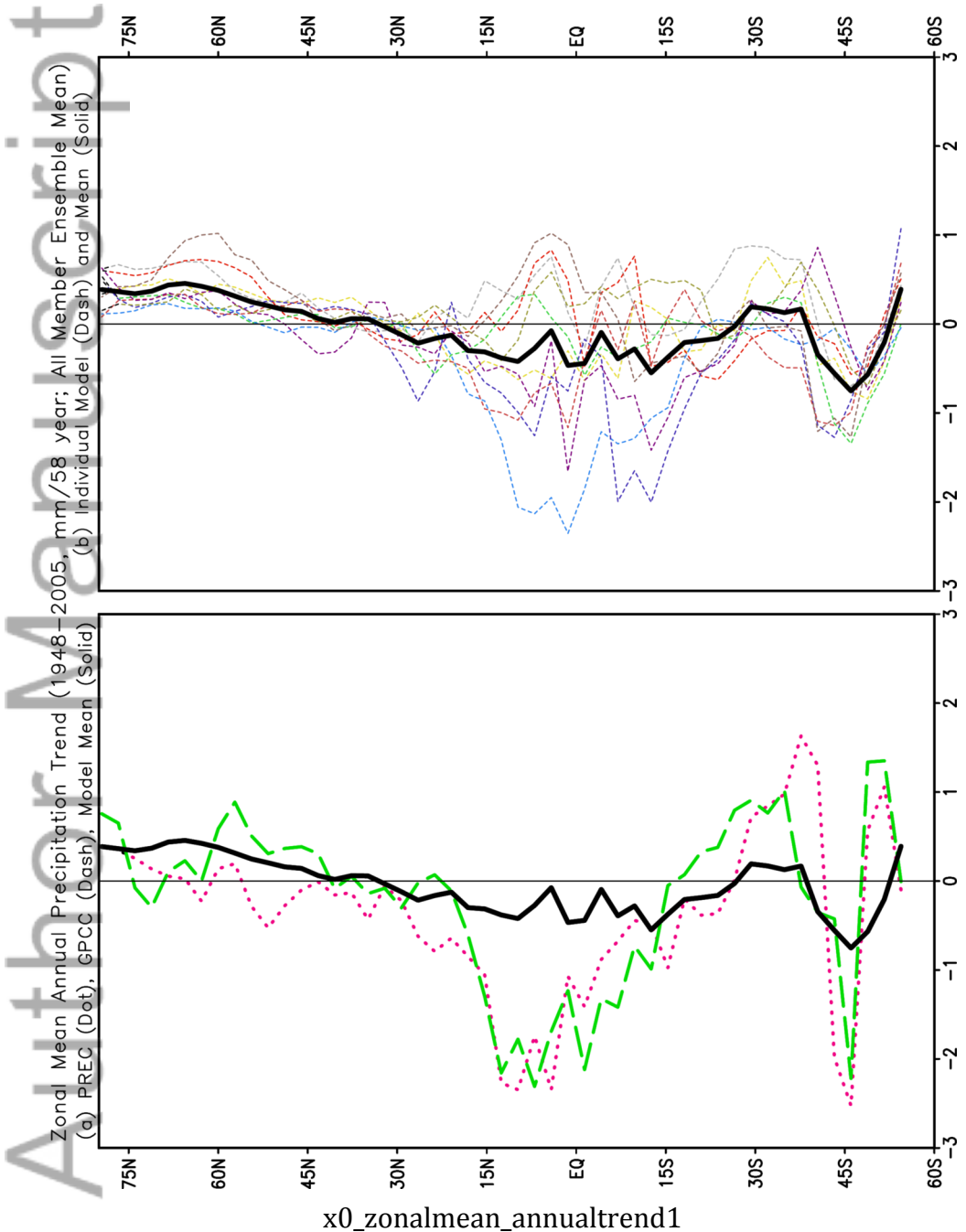

x0_zonalmean_annualtrend1

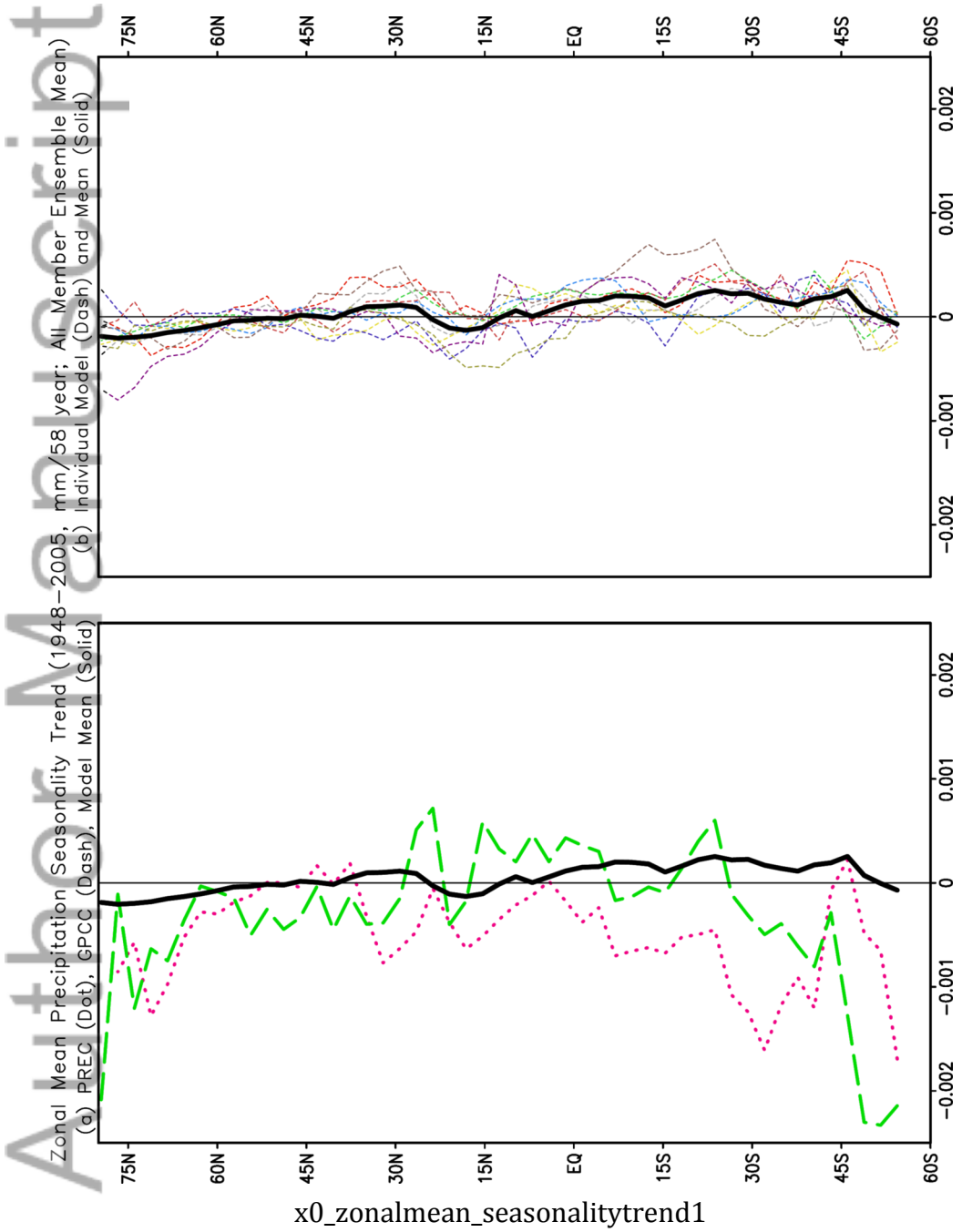

x0_zonalmean_seasonalitytrend1